THE ONE-DIMENSIONAL HUGHES MODEL FOR PEDESTRIAN FLOW: RIEMANN–TYPE SOLUTIONS

DEBORA AMADORI AND MARCO DI FRANCESCO

Dedicated to Professor Constantine M. Dafermos for his 70^{th} *birthday*

Abstract. This paper deals with a coupled system consisting of a scalar conservation law and an eikonal equation, called the Hughes model. Introduced in [24], this model attempts to describe the motion of pedestrians in a densely crowded region, in which they are seen as a 'thinking' (continuum) fluid. The main mathematical difficulty is the discontinuous gradient of the solution to the eikonal equation appearing in the flux of the conservation law. On a one dimensional interval with zero Dirichlet conditions (the two edges of the interval are interpreted as 'targets'), the model can be decoupled in a way to consider two classical conservation laws on two sub-domains separated by a *turning point* at which the pedestrians change their direction. We shall consider solutions with a possible jump discontinuity around the turning point. For simplicity, we shall assume they are locally constant on both sides of the discontinuity. We provide a detailed description of the local-in-time behavior of the solution in terms of a 'global' qualitative property of the pedestrian density (that we call 'relative evacuation rate'), which can be interpreted as the attitude of the pedestrians to direct towards the left or the right target. We complement our result with explicitly computable examples.

1. Introduction

In the recent years, the mathematical modeling of the behavior of human crowds has attracted considerate scientific interest. On the one hand this is due to its potential applications to the study of the dynamics of extraordinarily large groups of people in some concrete critical situations. The annual Hajj in Saudi Arabia and the recent Duisburg disaster in Germany in 2010 are very evocative examples in such sense. On the other hand, crowd management has important applications to structural engineering and architecture (cf. the London Millennium footbridge), transport systems, spectator occasions, political demonstrations, panic situations such as earthquakes and fire escapes, cf. [35].

The several approaches to the mathematical modeling of human crowds split into two main categories: discrete (microscopic) modeling and continuum (macroscopic) modeling. In the former approach, people are treated as individual entities (particles), the evolution of which is determined by physical and social laws which describe the interaction among the particles as well as their interactions with the physical surrounding, cf. [19, 32, 21], see also [20] and the references therein.

Date: November 15, 2011.
1991 *Mathematics Subject Classification.* 35L65, 35Q91.
Key words and phrases. pedestrian flow, nonlocal conservation law, eikonal equation.

The continuum approach usually deals with the crowd seen as a whole, without recognizing individual differences, and it is therefore more suited to the study of the movement of an extremely large number of pedestrians. Classical fluid–dynamics based approaches have been developed in [22, 23, 4]. More recent works are related with non classical mathematical tools such as gradient flows, cf. [31], optimal transport, cf. [8], time evolving measures, cf. [34]. 'Second order' (or hydrodynamical) models have been proposed in [2, 17]. Multiscale modeling of granular flows have been applied to this context in [13]. In [7], a model resembling the Keller–Segel system for chemotaxis has been derived as a limit of a cellular automation model used for simulating human crowds with herding behavior.

A more phenomenological (macroscopic) approach to pedestrian flow uses non classical variations to a scalar conservation law, in which the velocity field depends *non-locally* from the density of pedestrians on the whole domain. A first (modelling) significant attempt into this direction was performed by R. L. Hughes in [24, 25], based on the classical Witham–Lighthill approach for vehicular traffic flow, see [30]. In a multidimensional framework, the Hughes' model reads

$$\begin{cases} \dfrac{\partial \rho}{\partial t} - \mathrm{div}(\rho f^2(\rho)\nabla\phi) = 0 \\ f(\rho)|\nabla\phi| = 1. \end{cases} \tag{1}$$

The model is posed on a bounded domain in $\mathbb{R}^2$, with boundary conditions for the density ρ to be determined according to the practical circumstances. The function $f(\rho)$ decreases on an interval $[0,\rho_{max}]$ with $f(0) = v_{max} > 0$ and $f(\rho_{max}) = 0$. Roughly speaking, pedestrians are directed down the gradient of the potential ϕ which models the common sense of the target. The term $f(\rho)$ in the eikonal equation in (1) models the ability of the pedestrians to temper their estimated travel time by avoiding extremely high densities.

A more general model, still based on conservation laws with nonlocal velocity, was proposed by Bressan and Colombo in [6] and by Colombo and collaborators in [10], where a mathematical theory in the framework of entropy solutions has been developed. They propose a model of the form

$$\frac{\partial \rho}{\partial t} + \mathrm{div}(\rho f(\rho)(\nu(x) + \mathcal{I}(\rho)) = 0 \tag{2}$$

with ν an external velocity field and $\mathcal{I}(\rho(t))(x)$ being a vector field depending nonlocally on the density ρ, e.g. $\mathcal{I}(\rho(t))(x) = -\varepsilon \frac{\nabla(\rho(t)*\eta)}{\sqrt{1+|\nabla(\rho(t)*\eta)|^2}}$, η being a standard mollifier, $\varepsilon > 0$. Let us mention here that this structure is similar to the one proposed in [7] (in the latter, the nonlocal field is the gradient of the solution to a parabolic equation with a ρ-depending term in the reaction part). The framework developed in [10] covers maps $\mathcal{I} : L^1(\mathbb{R}^d;[0,R]) \to C^2(\mathbb{R}^d;\mathbb{R}^d)$, which allows to include a regularized version of the Hughes's model studied in [16], namely

$$\begin{cases} \dfrac{\partial \rho}{\partial t} - \mathrm{div}(\rho f^2(\rho)\nabla\phi) = 0 \\ -\varepsilon\Delta\phi + |\nabla\phi|^2 = \dfrac{1}{(f(\rho)+\varepsilon)^2}. \end{cases} \tag{3}$$

For (3), global existence and uniqueness of entropy solutions with bounded variations was first proven in [16] in one space dimension with homogeneous Dirichlet boundary conditions. The same result has been proven for the Cauchy problem in many dimensions as a consequence of the results in [10]. For the sake of completeness, let us also recall previous results in [11, 12] on a scalar conservation law with non classical shocks. Similar models are studied in [3] in the context of sedimentation models.

Our work deals with the original version of the Hughes model in one space dimension

$$\begin{cases} \rho_t - (\rho f^2(\rho)\phi_x)_x = 0 \\ f(\rho)|\phi_x| = 1, \end{cases} \tag{4}$$

posed on $x \in [-1, 1]$ with $f(\rho) = 1 - \rho$ (for more general assumptions on f, see (11)). Similarly to [16], we shall require the boundary conditions

$$\mathrm{Tr}\rho(t, \pm) \in [0, \frac{1}{2}] \tag{5}$$

$$\phi(t, \pm 1) = 0, \tag{6}$$

in which (5) should be interpreted as a zero Dirichlet condition, whereas (6) suggests that the boundary points are the target of the crowd.

The main difficulty in the study of (4) is the discontinuity of ϕ_x which depends non–locally on the density ρ. Such feature does not allow the use of previous studies on scalar conservation laws with discontinuous fluxes, cf. for instance [26]. The approximated procedure undertaken in [16] does not allow to pass into the limit since the estimates are not uniform with respect to the approximating parameter. Our strategy relies first on solving the eikonal equation in a semi–concave sense, which yields the existence of a unique discontinuity point for ϕ_x which we shall refer to as the *turning point* x_m of ρ. Then, we focus on the behavior of the solution ρ around the turning point (which depends on ρ in a non–local form). We provide 'local' exact solutions which are possibly discontinuous around the turning point, assuming for simplicity that they are locally constant on the two sides of the turning point. Our main result is stated in Theorem 1: we prove that the solution can exhibit several possible behaviors around the turning point depending on the global inertia of the crowd, which we shall call *relative evacuation rate*, see (29). In particular, either a vacuum region can be generated around x_m, or a intermediate value leading to a new (non classical) shock wave or to a new rarefaction wave. Although our result is valid only in one space dimension, it brings a new insight on this model which leads to quite natural interpretations, see for instance Remark 5.

The paper is structured as follows. In Section 2 we provide a precise statement of the problem (4), a suitable notion of solution, and we point out some basic properties of the solutions. In Section 3 we analyze the several possible behaviors of the density around the turning point, assuming that the initial density is locally constant on each side of x_m. In Section 4 we provide some examples.

2. Notions of solution and basic properties

We shall work on the model

$$\rho_t - (\rho f^2(\rho)\phi_x)_x = 0, \quad x \in [-1, 1], \quad t \geq 0 \tag{7}$$

$$f(\rho)|\phi_x| = 1, \quad x \in [-1, 1], \quad t \geq 0 \tag{8}$$

coupled with the initial condition

$$\rho(0, x) = \rho_0(x), \quad x \in [-1, 1], \qquad \rho_0(x) \in [0, 1) \tag{9}$$

and the boundary condition

$$\phi(t, \pm 1) = 0, \quad t \geq 0\,. \tag{10}$$

For future reference, we denote

$$g(\rho) = \rho f(\rho)\,.$$

On the function f we assume that

$$f \in C^2([0,1])\,, \quad f' < 0\,, \quad f(0) = 1\,, \quad f(1) = 0\,, \quad g \text{ is strictly concave}\,. \tag{11}$$

As an example, we will consider $f(\rho) = 1 - \rho$. Let $\bar{\rho}$ be the unique point in (0,1) where g attains its maximum. At the boundary $x = \pm 1$, we require that

$$\mathrm{Tr}\rho(t, \cdot) \in [0, \bar{\rho}], \quad x = \pm 1,\ t \geq 0. \tag{12}$$

The boundary condition (12) is justified as follows. The (possibly discontinuous) flux in the conservation law (7) is

$$\rho f^2(\rho)\phi_x = \rho f(\rho)\mathrm{sign}\phi_x = g(\rho)\mathrm{sign}\phi_x.$$

Therefore, the zero-Dirichlet boundary condition can be posed following [1] as follows:

$$\min_{k \in [0, \mathrm{Tr}\rho]} \left\{ - \left(g(\mathrm{Tr}\rho)\mathrm{sign}\phi_x(t,x) + g(k)\mathrm{sign}\phi_x(t,x) \right) \mathrm{sign}(x) \right\} = 0, \qquad \text{at } x = \pm 1. \tag{13}$$

As we shall see in Subsection 2.1, the eikonal equation (10) is solved in the sense of semi-concave solutions. Therefore, $\phi_x(-1,t) > 0$ and $\phi_x(1,t) < 0$, and the boundary condition (13) for ρ turns into

$$\min_{k \in [0, \mathrm{Tr}\rho]} \left(g(\mathrm{Tr}\rho) - g(k) \right) = 0, \qquad \text{at } x = \pm 1,$$

which easily yields the condition (12) because of the properties of g.

2.1. **Eikonal equation and turning point.** In this subsection we solve the eikonal equation (8) (and hence recast the whole problem (7)–(12)) in our one-dimensional framework.

Assume the density $\rho(t, \cdot)$ is known in the equation (8). For simplicity, let us assume that $\rho(t,x) \in [0, 1-\delta]$ for all $x \in [-1,1]$ and $t \geq 0$ for some $\delta > 0$. This ensures that one can rephrase (8) as

$$|\phi_x| = \frac{1}{f(\rho)} \tag{14}$$

and thus ϕ is a globally Lipschitz function on $[0,1]$.

It is well known from the standard theory of Hamilton-Jacobi type equations (see for instance [9]) that (14) may feature more than one weak solution. More precisely, there may be infinitely many points in $[-1,1]$ in which ϕ_x changes its sign (e.g. $1/f(\rho) = \text{constant}$). We shall opt for the (unique) solution with one single such point, namely $\phi_x > 0$ on some interval $[-1, x_m]$ and $\phi_x < 0$ on $[x_m, 1]$.

Such a choice can be motivated by the use of *semi-concave* solutions for (14), i. e. solutions ϕ such that ϕ_{xx} is bounded from above in the sense of distributions, see [9]. On the other hand, it can easily be motivated by physical considerations as follows.

The potential ϕ models the commons sense of the target by the pedestrians. Here the target consists in the boundary points $x = \pm 1$. It is reasonable to expect that ϕ will be increasing near $x = -1$ and decreasing near $x = 1$, which represents

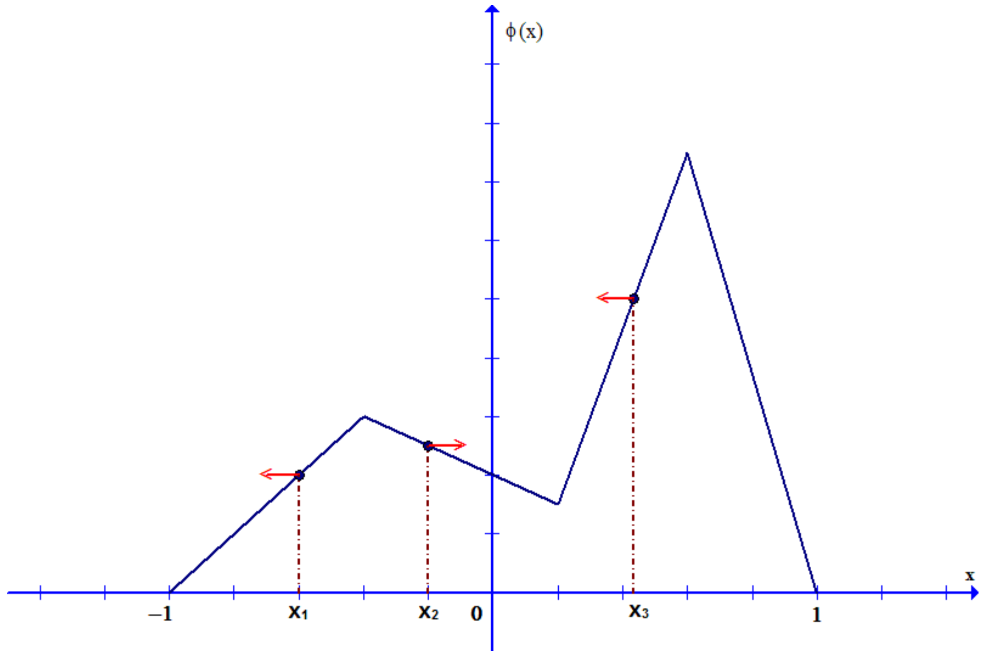

FIGURE 1. Non admissible solution to the eikonal equation (8)

the fact that pedestrians are directed towards a boundary point when they are very close to it. The natural question arises whether ϕ_x will change sign more than once over the interval $[-1, 1]$. Assume by contradiction that

$$\phi_x(x_1) > 0, \quad \phi_x(x_2) < 0, \quad \phi_x(x_3) > 0, \qquad \text{with } \ x_1 < x_2 < x_3,$$

for a given ρ, as illustrated in figure 1. As the velocity field is given by $V = (1-\rho)\text{sign}\phi_x$, then the pedestrians located at x_1, x_2, x_3 respectively are directed as in figure 1. This is a contradiction, since a pedestrian at x_2 cannot sense the target $x = 1$ closer than what the pedestrian located at x_3 does.

In view of the above argument, we shall consider solutions ϕ to the eikonal equation (14) with just one *turning point*, which we shall denote from now on as $x_m(t)$, such that

$$\phi_x(t, x) > 0 \quad \text{as } -1 < x < x_m(t), \qquad \phi_x(t, x) < 0 \quad \text{as } x_m(t) < x < 1. \tag{15}$$

The conservation law (7) can be then re-written as

$$\begin{cases} \rho_t - g(\rho)_x = 0 & \text{as } -1 < x < x_m(t) \\ \rho_t + g(\rho)_x = 0 & \text{as } x_m(t) < x < 1, \end{cases} \tag{16}$$

which implies that the flow is governed by two Witham-type equations with opposite directions on the two intervals $x < x_m(t)$ and $x > x_m(t)$.

Once we know that there exists only one turning point, we can explicitly solve the eikonal equation (8), with boundary condition (10), as follows:

$$\phi(t, x) = \begin{cases} \displaystyle\int_{-1}^{x} \frac{1}{f(\rho(t, y))} dy & \text{as } -1 < x < x_m(t) \\ \displaystyle\int_{x}^{1} \frac{1}{f(\rho(t, y))} dy & \text{as } x_m(t) < x < 1. \end{cases} \tag{17}$$

By the continuity of ϕ, we can use (17) to provide an implicit formula for the turning point $x_m(t)$:

$$\int_{-1}^{x_m(t)} \frac{1}{f(\rho(t,y))} dy = \int_{x_m(t)}^{1} \frac{1}{f(\rho(t,y))} dy. \tag{18}$$

Since $f > 0$ on $[0,1)$, then $x_m(t)$ in (18) is uniquely determined.

The formula (18) clarifies an essential property of the turning point $x_m(t)$, namely that $x_m(t)$ depends *non-locally* on the whole distribution of pedestrians $\rho(t)$ on $[-1,1]$. In particular, the turning point is automatically determined by the initial datum ρ_0 at time $t = 0$, via the formula

$$\int_{-1}^{x_m(0)} \frac{1}{f(\rho_0(y))} dy = \int_{x_m(0)}^{1} \frac{1}{f(\rho_0(y))} dy. \tag{19}$$

2.2. **Entropy solution.** In view of the considerations in the subsection 2.1, the conservation law (7) can be split in two separate conservation laws as in (16). Therefore, ρ evolves according to the classical theory (see [5, 15] for instance) away from the turning point, i. e. on the domains $x < x_m(t)$ (convex flux $-g$) and $x > x_m(t)$ (concave flux g). It is well known that the Cauchy problem to a scalar conservation law may feature, in general, more than one weak solution, which yields the need for the (stronger) concept of entropy solution, cf. [33, 27]. In our case, the well known Lax admissibility criterion for shocks [29] implies that admissible shocks are decreasing on $x < x_m(t)$ and increasing on $x > x_m(t)$.

We are now ready to define our notion of entropy solution for (7)–(12).

Definition 1 (Weak entropy solutions)**.** *Let* $0 < \delta < 1$ *and* $\rho_0 \in BV \cap L^\infty([-1,1])$ *with* $\rho_0(x) \in [0, 1-\delta]$. *A function* $\rho(x,t) \in L^\infty \cap BV_{loc}([0,+\infty) \times [-1,1])$ *is a BV* weak entropy solution *to the problem* (7)–(8)–(10)–(12) *with initial datum* ρ_0 *if and only if* $\rho(t,x) \in [0, 1-\delta]$ *for all* $x \in [-1,1]$ *and* $t \geq 0$, *and the following conditions are satisfied:*

(1) For all test functions $\varphi \in C_c^\infty([0,T) \times (-1,1))$ *we have*

$$\int_0^T \int_{-1}^1 \rho(t,x)\varphi_t(t,x) dx dt + \int_{-1}^1 \rho_0(x)\varphi(0,x) dx$$
$$- \int_0^T \int_{-1}^1 g(\rho(t,x)) \mathrm{sign}(x_m(t) - x)\varphi_x(t,x) dx dt = 0, \tag{20}$$

where $x_m(t)$ *is defined by* (18)*;*

(2) $\mathrm{Tr}\rho(t, x = \pm 1) \in [0, \bar{\rho}]$ *for all* $t > 0$.

(3) For each convex function $e : [0, 1-\delta] \mapsto \mathbb{R}$ *there exists a Lipschitz function* $p : [0, 1-\delta] \mapsto \mathbb{R}$ *such that*

$$\begin{cases} e(\rho)_t - p(\rho)_x \leq 0 & \text{on} \quad x < x_m(t) \\ e(\rho)_t + p(\rho)_x \leq 0 & \text{on} \quad x > x_m(t) \end{cases} \tag{21}$$

where both the above inequalities are satisfied in the sense of distributions.

As usual in this framework, we shall call e *entropy* and p *entropy flux.*

Remark 1 (Justification of the assumptions in Definition 1)**.** The BV condition is required here for two reasons. On the one hand, in this paper we shall provide a class of exact solutions with finite left and right limit for $\rho(t,\cdot)$ for all $t \geq 0$. On the other hand, we conjecture (see Conjecture 1) that the initial finiteness of the total variation is propagated along the solution. This issue is strictly related with the effectiveness of the wave front tracking strategy for this problem (cf. [14]), which is the topic of a parallel work by the authors.

The condition $\rho \leq 1-\delta$ for all $t \geq 0$ is used to avoid the singularity in (14), due to the condition $f(1) = 0$ (i.e., null velocity at maximum density). We assume this condition on the initial data and expect that, by maximum principle, it is satisfied at later times: $\|\rho(t)\|_{L^\infty} \leq \|\rho_0\|_{L^\infty}$ for all $t \geq 0$. The Riemann–type solutions considered in Theorem 1 do satisfy this property.

The behavior of the solution at the boundary points $x = \pm 1$ can be determined as in [18], by solving two Riemann problems: at $x = -1$ with $\rho_- = 0$ and $\rho_+ = \mathrm{Tr}(\rho(x = -1))$, at $x = 1$ with $\rho_- = \mathrm{Tr}(\rho(x = 1))$ and $\rho_+ = 0$. Since g is concave, the two boundary layers at $x = \pm 1$ have to be solved by means of a *rarefaction wave*. The rarefaction fan generated at the boundary *enters* the domain $[-1, 1]$ when the trace of ρ (on both sides $x = \pm 1$) satisfies $\mathrm{Tr}(\rho) \in [\bar{\rho}, 1]$ and *leaves* the domain otherwise.

For now on we shall denote

$$\eta(\rho) := \frac{1}{f(\rho)}.$$

Notice that $\eta'(\rho) = -f'(\rho)/f(\rho)^2$ and therefore η is strictly increasing on $[0, 1)$ with $\eta(\rho) \to +\infty$ as $\rho \nearrow 1^-$.

Remark 2 (Entropy solutions and semi-concave functions)**.** As we noticed before, the notion of entropy solution for (16) (cf. [28]) implies that admissible shocks are decreasing for $x < x_m(t)$ and increasing for $x > x_m(t)$. This fact is compatible with the semi–concavity of ϕ with a unique turning point chosen in (15). Indeed, since all the jumps of ρ on $x < x_m(t)$ are decreasing, the same holds for $\eta(\rho) = \phi_x$ because η is a strictly increasing function of ρ. Hence, the measure ϕ_{xx} is locally bounded from above in $\mathcal{D}'$. Similarly, one can prove that the measure $-\phi_{xx}$ is bounded from below in $\mathcal{D}'$ on $x > x_m(t)$. At $x = x_m(t)$, ϕ_x has a decreasing jump, which proves the assertion.

The major difference with respect to the classical conservation law theory is the presence of the turning point $x_m(t)$, which determines a discontinuity in the flux and which depends non-locally on $\rho(\cdot, t)$. In the computations we shall perform in this paper, it will be useful to have the turning point curve $t \mapsto x_m(t)$ locally Lipschitz. A reasonable sufficient condition for that is the time continuity of the L^1 semigroup, which is usually satisfied in the classical theory, cf. [5].

Proposition 1. *Assume that ρ is a weak entropy solution according to Definition 1, with corresponding turning point curve $x_m(t)$. Assume further that*

$$\|\rho(\cdot, t) - \rho(\cdot, s)\|_{L^1([-1,1])} \leq C|t - s|, \tag{22}$$

for some constant $C > 0$ depending only on the function f and on the initial datum. Then, the turning point curve $x_m(t)$ is Lipschitz on $[0, +\infty)$.

Proof. Due to (18), we have

$$\int_{-1}^{x_m(t)} \eta(\rho(t, x))dx - \int_{-1}^{x_m(s)} \eta(\rho(s, x))dx = \int_{x_m(t)}^{1} \eta(\rho(t, x))dx - \int_{x_m(s)}^{1} \eta(\rho(s, x))dx$$

which yields

$$2|x_m(t) - x_m(s)| = 2\left|\int_{x_m(s)}^{x_m(t)} \eta(\rho(t,x))dx\right|$$
$$\leq \int_{-1}^{x_m(s)} |\eta(\rho(t,x)) - \eta(\rho(s,x))|\, dx + \int_{x_m(s)}^{1} |\eta(\rho(t,x)) - \eta(\rho(s,x))|\, dx. \quad (23)$$

Since the function $\rho \mapsto \eta(\rho)$ has Lipschitz constant equal to $C(f,\delta) := \frac{\|f'\|_{L^\infty([0,1])}}{f(1-\delta)^2}$ on the interval $\rho \in [0, 1-\delta]$, we have

$$\left|\int_{-1}^{x_m(s)} [\eta(\rho(t,x)) - \eta(\rho(s,x))]\, dx\right| \leq C(f,\delta)\int_{-1}^{x_m(s)} |\rho(x,t) - \rho(x,s)|dx \quad (24)$$

which coupled with (23) and (22) gives the desired assertion. □

From now on in the paper we shall assume the turning point curve $t \mapsto x_m(t)$ is Lipschitz, which implies it is differentiable almost everywhere. We shall see in Section 4 that the Lipschitz regularity for $x_m(t)$ is sharp, namely we shall produce examples in which $\dot{x}_m(t)$ is discontinuous.

In the classical conservation laws theory the speed of propagation of a discontinuity can be made explicit in terms of the right and left states via the Rankine–Hugoniot condition, cf. [5, 15]. Clearly, in our case all discontinuities can be treated as in the classical case (see also [36]) *away* from the turning point.

Assume now that a discontinuity along the turning point curve $t \mapsto x_m(t)$ occurs, with ρ_L and ρ_R being the left and right limit respectively. Then, the usual computations leading to the Rankine–Hugoniot conditions yield

$$(\rho_R - \rho_L)\dot{x}_m(t) = g(\rho_R) + g(\rho_L). \quad (25)$$

Notice that (25) makes sense even in the case $\rho_L = \rho_R$. In this circumstance, since $\dot{x}_m$ finite, it implies that $g(\rho_R) = 0$, that is either $\rho_R = 0$ or $\rho_R = 1$. However, we notice that $\rho_R = 1$ violates Definition 1, therefore we shall only deal with $\rho_R = 0$.

Now we analyze the solution to (25) in the case of $\dot{x}_m(t) = \lambda$, with $\lambda \in \mathbb{R}$ given. This will be used in the construction of the Riemann solver around the turning point.

Let $\rho_L \in [0,1)$. We want to determine for which $\lambda \in \mathbb{R}$ the equation

$$(\rho_R - \rho_L)\lambda \quad = \quad g(\rho_R) + g(\rho_L)\,, \qquad \rho_R \in [0,1) \quad (26)$$

has a solution, possibly unique. If $\rho_L = 0$, then (26) is satisfied for

- $\rho_R = 0$, for all λ
- $\rho_R \in (0,1)$, $\lambda = 1 - \rho_R \in (0,1)$.

On the other hand, if $\rho_L > 0$, we set $x = \rho_L$, $y = \rho_R$. For $x = y > 0$ there are no solutions. For $x \neq y$, it is easy to compute that the range of

$$[0,1) \setminus \{x\} \ni y \mapsto \frac{g(y) + g(x)}{y - x}$$

is given by $(-\infty, -(1-x)] \cup (x, \infty)$. Moreover

$$\frac{\partial}{\partial y}\frac{g(y)+g(x)}{y-x} \quad = \quad -\frac{1}{(y-x)^2}\left[g'(y)(x-y) + g(y) + g(x)\right] \;\leq\; -\frac{2g(x)}{(y-x)^2} < 0$$

because of the concavity of g. Hence the solution to (26) for $\rho_L > 0$, whenever it exists for a certain λ, it is unique.

We have therefore proven the following Proposition:

Proposition 2 (Rankine–Hugoniot condition around the turning point). *Let $\rho(t,x)$ be a BV weak entropy solution according to Definition 1 which is possibly discontinuous along the (Lipschitz) turning curve $[t_1,t_2] \in t \mapsto x_m(t)$. Let $t \in [t_1,t_2]$ and let ρ_L and ρ_R be the left and right limit of $\rho(t)$ at $x_m(t)$ respectively. Then, one of the following two situations occurs:*

(1) $\rho_L = \rho_R = 0$ and $\dot{x}_m(t)$ is not determined by (25),
(2) $\rho_L \neq \rho_R$ and

$$\dot{x}_m(t) = \lambda(\rho_L, \rho_R) := \frac{g(\rho_R) + g(\rho_L)}{\rho_R - \rho_L} \,. \tag{27}$$

In particular,

- *If $\rho_L < \rho_R$ then $\lambda(\rho_L,\rho_R) \in [\rho_L, +\infty)$.*
- *If $\rho_L > \rho_R$ then $\lambda(\rho_L,\rho_R) \in (-\infty, -(1-\rho_L)]$.*

Moreover, assuming ρ_L fixed and $\dot{x}_m(t) = \lambda$ fixed, there exists a unique ρ_R such that (25) holds.

Conjecture 1. We conjecture that an existence theorem for entropy solutions according to Definition 1 can be performed. This is the subject of a work in preparation by the authors, which uses the wave front tracking strategy, cf. [14]. We also conjecture the uniqueness of entropy solutions due to the fact that no dichotomy between shocks and rarefaction seems to occur at the turning point. Indeed, we can see from Proposition 2 that the only possibility for a continuous solution around the turning point is that of a vacuum formation. On the other hand, the computations in the rest of the paper show how to detect the behavior of the solution around the turning point in a unique way in a quite general framework. As for the condition $\rho \leq 1-\delta$ for all $t \geq 0$ in Definition 1, this property is clearly preserved away from x_m; on the other hand, the result in Theorem 1 suggests that it is also propagated along the turning point.

2.3. **An additional condition on $\dot{x}_m(t)$.** In this subsection we state a key condition we shall need in order to find a suitable solution around the turning point $x_m(t)$. The case $\rho_L = \rho_R = 0$ in Proposition 2 shows in fact that the Rankine–Hugoniot condition (25) may not be sufficient to determine the speed $\dot{x}_m(t)$ of the turning point. Unlike the classical case, we shall see that when a discontinuity appears around the turning point - e.g. at time $t = 0$ - the two traces ρ_L and ρ_R of the solution around $x_m(t)$ at $t > 0$ *may be not both equal to the traces at $t = 0$*. This fact suggests that the Rankine–Hugoniot condition (25) should be complemented with some additional condition.

Formally, the speed of the turning curve $\dot{x}_m$ can be deduced by taking the time derivative in (18) as follows. By denoting the traces $\rho(t, x_m(t)-) = \rho_L$ and $\rho(t, x_m(t)+) = \rho_R$, from (18) we deduce

$$\dot{x}_m \left[\eta\left(\rho_L\right) + \eta\left(\rho_R\right)\right] = \left\{ \int_{x_m(t)}^{1} - \int_{-1}^{x_m(t)} \right\} \partial_t [\eta\left(\rho(t,y)\right)] dy \,. \tag{28}$$

Remark 3. Let us recall that, although $\partial_t \eta(\rho)$ might be not well defined in case of jumps, the terms $\int_{-1}^{x_m(t)} \partial_t \eta(\rho(x,t)) dx$ and $\int_{x_m(t)}^{1} \partial_t \eta(\rho(x,t)) dx$ make sense if ρ is a

BV solution in the sense of Definition 1. In particular, assume that ρ has a finite number of jumps and it is differentiable elsewhere for all $t \geq 0$. A discontinuity along the shock curve $t \mapsto s(t) \in [-1, x_m(t))$ with ρ_ℓ and ρ_r left and right traces respectively produces a contribution of the form

$$\dot{s}(t)(\eta(\rho_\ell) - \eta(\rho_r))$$

to the integral term $\int_{-1}^{x_m(t)} \partial_t \eta(\rho(x,t))dx$. On an interval $[a,b]$ on which ρ is differentiable, we have to compute the *flux* function $q(\rho)$, namely

$$q'(\rho) = \eta'(\rho)g'(\rho) = -\frac{f'(\rho)(\rho f'(\rho) + f(\rho))}{f(\rho)^2}\,,$$

which yields

$$q(\rho) = \frac{\rho f'(\rho)}{f(\rho)} - 2\log f(\rho) - \int^{\rho} \frac{\xi f''(\xi)}{f(\xi)} d\xi\,.$$

Hence,

$$\int_a^b \partial_t \eta(\rho(x,t))dx = \int_a^b q(\rho)_x dx = q(b) - q(a), \qquad \text{if } \ a < b < x_m(t)$$

$$\int_a^b \partial_t \eta(\rho(x,t))dx = -\int_a^b q(\rho)_x dx = -q(b) + q(a), \qquad \text{if } \ x_m(t) < a < b$$

We shall use the notation

$$\Psi[\rho](t) := \left\{ \int_{x_m(t)}^1 - \int_{-1}^{x_m(t)} \right\} \partial_t [\eta\left(\rho(t,y)\right)] dy\,, \tag{29}$$

which means that (28) can be rephrased as

$$\dot{x}_m \left[\eta\left(\rho_\ell\right) + \eta\left(\rho_r\right)\right] = \Psi[\rho](t). \tag{30}$$

The quantity $\Psi[\rho](t)$ is called *relative evacuation rate of* ρ *at the turning point.* For a given distribution of pedestrians $\rho(t,\cdot)$, $\Psi[\rho](t)$ measures somehow the balance between the trend towards the left or to the right edge of the interval $[-1,1]$ for those pedestrians located at the turning point: $\Psi[\rho](t) = 0$ means that the two edges are 'felt' at the same distance on $x = x_m(t)$, whereas $\Psi[\rho](t) > 0$ ($\Psi[\rho](t) < 0$ resp.) means that $x = -1$ is felt closer (farther) than $x = 1$ at $x = x_m(t)$.

Remark 4. The choice for the notation of Ψ is justified by following observation: assume for simplicity that ρ is smooth on the two intervals $x \in [-1, x_m(t))$ and $x \in (x_m(t), 1]$ separately. Then, due to (14)

$$\begin{aligned} &\left\{ \int_{x_m(t)}^1 - \int_{-1}^{x_m(t)} \right\} \partial_t [\eta\left(\rho(t,y)\right)] dy = -\int_{x_m(t)}^1 \phi_{xt} dx - \int_{-1}^{x_m(t)} \phi_{xt} dx \\ &= \phi_t(t, x_m(t)+) - \phi_t(t, x_m(t)-). \end{aligned} \tag{31}$$

Now, heuristically speaking, the term $\phi_t(t, x_m(t)+)$ is nonnegative when the individuals on the right–hand side of the turning point 'sense' the distance to the boundary $x = 1$ to increase, which is a reason why they rather prefer to turn towards the left–hand side. A symmetric interpretation holds for the term $\phi_t(t, x_m(t)-)$.

According to Proposition 2, two situations can occur:

(1) $\rho_L = \rho_R = 0$. In this case (28) just simplifies to

$$2\dot{x}_m = \left\{ \int_{x_m(t)}^{1} - \int_{-1}^{x_m(t)} \right\} \partial_t[\eta\left(\rho(t,y)\right)]dy = \Psi[\rho](t)\,. \tag{32}$$

(2) $\rho_L \neq \rho_R$. Here the Rankine–Hugoniot condition (25) gives an extra relation for $\dot{x}_m(t)$, and the following condition must hold:

$$\frac{g(\rho_L)+g(\rho_R)}{\rho_R-\rho_L}\left[\eta(\rho_L)+\eta(\rho_R)\right] = \left\{ \int_{x_m(t)}^{1} - \int_{-1}^{x_m(t)} \right\} \partial_t[\eta\left(\rho(t,y)\right)]dy = \Psi[\rho](t)\,. \tag{33}$$

Condition (33) is of paramount importance in order to determine the behavior of the solution around the turning point, as we shall point out in Section 3.

3. Solution around the turning point

In this section we consider a Riemann-type initial data and look for a local in time solution as in Definition 1. We will describe, specifically, how the solution evolves around the turning point.

We assume that the initial data ρ_0 is BV on $[-1,1]$ and that

$$\rho_0(x) = \begin{cases} \rho_L & \text{if } x_m(0) - 2\delta < x < x_m(0), \\ \rho_R & \text{if } x_m(0) < x < x_m(0) + 2\delta \end{cases} \tag{34}$$

for some $\delta > 0$ and $\rho_L,\ \rho_R \in [0,1)$. As before, $x = x_m(0)$ denotes the location of the turning point at $t = 0$, determined by (19), which we recall here for simplicity:

$$\int_{-1}^{x_m(0)} \eta\left(\rho_0(y)\right)\, dy = \int_{x_m(0)}^{1} \eta\left(\rho_0(y)\right)\, dy\,.$$

Recalling (16), the solution $\rho(t,x)$ is well defined far from the turning point, say on $[-1, x_m(0)-\delta) \cup (x_m(0)+\delta, 1]$, for $t > 0$ sufficiently small. Therefore, the following quantity is well defined

$$\left\{ \int_{x_m(0)+\delta}^{1} - \int_{-1}^{x_m(0)-\delta} \right\} \partial_t[\eta\left(\rho(t,y)\right)]dy \quad =: \quad \Psi^*\,.$$

In the following we will assume that Ψ^* is constant, for small positive times. As a consequence, the solution around the turning point will be self-similar, behaving as a solution of a Riemann problem. This assumption is met when there are no interacting patterns; we will show some examples in the next Section. Therefore, for small times we have

$$\Psi[\rho] \quad = \quad \Psi^* + \left\{ \int_{x_m(t)}^{x_m(0)+\delta} - \int_{x_m(0)-\delta}^{x_m(t)} \right\} \partial_t[\eta\left(\rho(t,y)\right)]dy\,. \tag{35}$$

The term Ψ^* depends on the initial data in a nonlocal way and may range all over $\mathbb{R}$, independently of ρ_L and ρ_R. The solution around $x_m(0)$ will be classified according to the value of Ψ^*.

Theorem 1. *Assume that $\rho_L > \rho_R$. If (34) and (35) hold, then a self-similar solution around $(0, x_m(0))$ is defined locally in time, and the following cases occur.*

(a) *If*
$$\Psi^* < \frac{g(\rho_R)+g(\rho_L)}{\rho_R-\rho_L}\left[\eta(\rho_R)+\eta(\rho_L)\right] , \tag{36}$$
then there exists a unique intermediate value ρ_m*, with* $\rho_L > \rho_m > \rho_R$*, such that the solution is given by the turning curve* x_m *followed by a rarefaction between* ρ_m *and* ρ_R*.*

(b) *If*
$$\frac{g(\rho_R)+g(\rho_L)}{\rho_R-\rho_L}\left[\eta(\rho_R)+\eta(\rho_L)\right] \;\le\; \Psi^* \;\le\; -\left[f(\rho_L)+f(\rho_R)\right] , \tag{37}$$
then a unique intermediate a value $\rho_m \in [0,\rho_R]$ *exists, such that the solution is given by the turning curve* x_m *followed by a shock between* ρ_m *and* ρ_R*.*

If the equality holds in the r.h.s. of (37)*, then* $\rho_m = 0$*: vacuum appears between the turning point and the shock.*

(c) *If*
$$|\Psi^*| \;<\; f(\rho_L)+f(\rho_R) \tag{38}$$
then the solution is given by a shock x_L *followed by* x_m *and by a shock* x_R*, the intermediate state being* $\rho = 0$*. That is,* $x_L(t) < x_m(t) < x_R(t)$*.*

(d) *Finally if*
$$\Psi^* \;\ge\; f(\rho_L)+f(\rho_R) \tag{39}$$
then the solution is given by a shock x_L *followed by* x_m*, the intermediate state being* $\rho_m \in [0,\rho_R)$*. If equality holds in* (39)*, then* $\rho_m = 0$*, otherwise* $\rho_m > 0$*.*

Before proving the Theorem we mention that a similar statement holds for $\rho_L < \rho_R$, while for $\rho_L = \rho_R$ (hence, the initial data is continuous at $x = x_m(0)$) condition (36) loses its meaning, since the r.h.s. goes to $-\infty$, and the other conditions have a natural counterpart. The proofs are completely analogous to the one of the Theorem.

Note also that an increase of the total variation occurs in cases (b), (c) and (d).

Proof. We start by observing that, for $\rho_R < \rho_L$, the condition given in (37) is meaningful. Indeed, we need to verify that
$$\frac{g(\rho_L)+g(\rho)}{\rho_L-\rho}\left[\eta(\rho_L)+\eta(\rho)\right] \quad\ge\quad f(\rho_L)+f(\rho) , \qquad \rho\in[0,\rho_L) . \tag{40}$$
To prove it, consider
$$[0,\rho_L)\ni\rho \;\mapsto\; \Phi(\rho) \;:=\; \frac{g(\rho_L)+g(\rho)}{\rho_L-\rho}\left[\eta(\rho_L)+\eta(\rho)\right] - f(\rho) .$$
Recalling that $g(\rho) = \rho f(\rho)$, $\eta(\rho) = 1/f(\rho)$ and that $f(0) = 1$, it is immediate to verify that equality in (40) holds for $\rho = 0$ and that $\Phi(\rho)\to+\infty$ as $\rho\to\rho_L$.

We claim that $\Phi'(\rho) > 0$, which is enough to conclude. Rewrite Φ as
$$\Phi(\rho) \quad=\quad \frac{g(\rho)}{\rho_L-\rho}\eta(\rho_L) + \frac{\eta(\rho)}{\rho_L-\rho}g(\rho_L) + \frac{\rho_L+\rho}{\rho_L-\rho} - f(\rho) .$$

Then

$$\begin{aligned}\Phi'(\rho) &= \frac{g'(\rho)(\rho_L-\rho)+g(\rho)}{(\rho_L-\rho)^2}\eta(\rho_L)+\frac{\eta'(\rho)(\rho_L-\rho)+\eta(\rho)}{(\rho_L-\rho)^2}g(\rho_L)\\ &\quad+\frac{2\rho_L}{(\rho_L-\rho)^2}-f'(\rho)\\ &\geq \frac{g(\rho_L)\eta(\rho_L)}{(\rho_L-\rho)^2}>0\,,\end{aligned}$$

where we have used that g is concave and that η, η', $-f'$ are positive.

Let us denote by ρ_L^* and ρ_R^* the left and right state along the turning point $x_m(t)$. Recalling Rankine–Hugoniot condition (25), the following condition must be satisfied:

$$(\rho_R^*-\rho_L^*)\dot{x}_m = g(\rho_R^*)+g(\rho_L^*)\,. \tag{41}$$

Recalling (32) and (33), two situations can occur: either (1) $\rho_L^*=\rho_R^*=0$ or (2) $\rho_L^*\neq\rho_R^*$. We analyze them in more detail.

(1) $\rho_L^*=\rho_R^*=0$. Recalling (16), on the left of x_m one has to match the values ρ_L and $\rho=0$. Since the flux is convex, this is obtained with a shock, whose speed is $-g(\rho_l)/\rho_L=-f(\rho_L)$.

Similarly, on the right of x_m the flux is concave and a shock connects $\rho=0$ to $\rho=\rho_R$, with speed $f(\rho_R)$.

Denote by $x_L(t)$ and $x_R(t)$ the two shocks, respectively at the left and right of the turning point. The propagation speed of the turning point is given by (28) that rewrites as

$$\begin{aligned}2\dot{x}_m &= \Psi[\rho]=\Psi^*+\left\{\int_{x_m(t)}^{x_m(0)+\delta}-\int_{x_m(0)-\delta}^{x_m(t)}\right\}\partial_t[\eta\left(\rho(t,y)\right)]dy\\ &= \Psi^*-\dot{x}_L\left[\eta(\rho_L)-\eta(0)\right]+\dot{x}_R\left[\eta(0)-\eta(\rho_R)\right]\\ &= \Psi^*+f(\rho_R)-f(\rho_L)\,.\end{aligned}$$

Finally, we impose the natural condition

$$\dot{x}_L<\dot{x}_m<\dot{x}_R \quad\Rightarrow\quad -f(\rho_L)<\frac{1}{2}\left\{\Psi^*+f(\rho_R)-f(\rho_L)\right\}<f(\rho_R)$$

that is satisfied if and only if (38) holds. Hence (c) is proved.

(2) $\rho_L^*\neq\rho_R^*$. We first look for a solution of type (b): the turning point x_m followed by a shock, located at x_R. Hence we seek an intermediate value $\rho_m\in[0,\rho_R)$. Here $\rho_L^*=\rho_L$ and $\rho_R^*=\rho_m$.

Therefore we have the following three conditions on $\dot{x}_m$:

(i) the Rankine–Hugoniot condition (41),

(ii) $\dot{x}_m<\dot{x}_R=\frac{g(\rho_R)-g(\rho_m)}{\rho_R-\rho_m}$

(iii) condition (28), that gives

$$\dot{x}_m\left[\eta(\rho_L)+\eta(\rho_m)\right] = \Psi^*+\dot{x}_R\left[\eta(\rho_m)-\eta(\rho_R)\right]\,.$$

We notice that (ii) is satisfied, since from (41) one has

$$\dot{x}_m=\frac{g(\rho_m)+g(\rho_L)}{\rho_m-\rho_L} < \frac{g(\rho_m)-g(\rho_L)}{\rho_m-\rho_L} < \frac{g(\rho_m)-g(\rho_R)}{\rho_m-\rho_R}=\dot{x}_R\,,$$

where we used that $\rho_m<\rho_R<\rho_L$ and the concavity of g.

From condition (iii) and setting $\rho = \rho_m$, we get

$$\theta(\rho) := \underbrace{\frac{g(\rho)+g(\rho_L)}{\rho-\rho_L}\left[\eta(\rho)+\eta(\rho_L)\right]}_{\theta_1(\rho)} \underbrace{-\frac{g(\rho)-g(\rho_R)}{\rho-\rho_R}\left[\eta(\rho)-\eta(\rho_R)\right]}_{\theta_2(\rho)} \quad = \quad \Psi^*\,.$$

By straightforward computations, we find

$$\theta(0) = -[f(\rho_L)+f(\rho_R)]\,, \qquad \theta(\rho_R) = \frac{g(\rho_R)+g(\rho_L)}{\rho_R-\rho_L}\left[\eta(\rho_R)+\eta(\rho_L)\right]\,.$$

We claim that $\theta'(\rho) \le 0$, which is enough to conclude the proof of case (b). Indeed, by the concavity of g we have

$$\begin{aligned}
\theta_1'(\rho) &= (g'(\rho)(\rho-\rho_L)-g(\rho)-g(\rho_L))\,\frac{\eta(\rho_L)+\eta(\rho)}{(\rho-\rho_L)^2} \;+\; \frac{g(\rho)+g(\rho_L)}{\rho-\rho_L}\eta'(\rho)\\
&\le -2g(\rho_L)\frac{\eta(\rho_L)+\eta(\rho)}{(\rho-\rho_L)^2} \;+\; \frac{g(\rho)+g(\rho_L)}{\rho-\rho_L}\eta'(\rho)\\
&\le \frac{g(\rho)+g(\rho_L)}{\rho-\rho_L}\eta'(\rho)\,.
\end{aligned}$$

Again by the concavity of g, since η increasing, and since $\rho \le \rho_R < \rho_L$ we have

$$\begin{aligned}
\theta_2'(\rho) &= (g'(\rho)(\rho-\rho_R)-g(\rho)+g(\rho_R))\,\frac{\eta(\rho_R)-\eta(\rho)}{(\rho-\rho_R)^2} \;-\; \frac{g(\rho)-g(\rho_R)}{\rho-\rho_R}\eta'(\rho)\\
&\le -\frac{g(\rho)-g(\rho_R)}{\rho-\rho_R}\eta'(\rho) \;\le\; -\frac{g(\rho)-g(\rho_L)}{\rho-\rho_L}\eta'(\rho).
\end{aligned}$$

Hence, summing up we get

$$\theta'(\rho) \le \frac{g(\rho)+g(\rho_L)}{\rho-\rho_L}\eta'(\rho) - \frac{g(\rho)-g(\rho_L)}{\rho-\rho_L}\eta'(\rho) = 2\frac{g(\rho_L)}{\rho-\rho_L}\eta'(\rho).$$

Since $\rho < \rho_L$, we end up with $\theta'(\rho) \le 0$.

Now we look for a solution of type (a): the turning point x_m followed by a rarefaction. Hence we seek an intermediate value $\rho_m > \rho_R$. Here condition (28) rewrites as

$$\begin{aligned}
\dot{x}_m\left[\eta(\rho_L)+\eta(\rho_m)\right] &= \Psi^* + \int_{x_m(t)}^{x_m(0)+\delta} \partial_t[\eta\left(\rho(t,y)\right)]dy\\
&= \Psi^* - \int_{x_m(t)}^{x_m(0)+\delta} \partial_x[q\left(\rho(t,y)\right)]dy\\
&= \Psi^* - q(\rho_R) + q(\rho_m)\,.
\end{aligned}$$

Therefore we have to determine $\rho > \rho_R$ such that

$$\xi(\rho) := \frac{g(\rho)+g(\rho_L)}{\rho-\rho_L}\left[\eta(\rho_L)+\eta(\rho)\right] + q(\rho_R) - q(\rho) \quad = \quad \Psi^*\,.$$

It is immediate to verify that $\xi(\rho)$ tends to $-\infty$ as $\rho \to \rho_L-$, and that $\xi(\rho_R)$ equals to the r.h.s. of (36). It remains to prove that $\xi' \leq 0$. Let us compute

$$\begin{aligned}\xi'(\rho) = &\frac{1}{(\rho-\rho_L)^2}\left[g'(\rho)(\rho-\rho_L) - g(\rho) - g(\rho_L)\right](\eta(\rho_L)+\eta(\rho)) \\ &+ \frac{g(\rho)+g(\rho_L)}{\rho-\rho_L}\eta'(\rho) - g'(\rho)\eta'(\rho) \\ &\leq -\frac{2g(\rho_L)(\eta(\rho_L)+\eta(\rho))}{(\rho-\rho_L)^2} - 2\frac{g(\rho_L)}{\rho_L-\rho}\eta'(\rho) \\ &+ \frac{g(\rho)-g(\rho_L)}{\rho-\rho_L}\eta'(\rho) - g'(\rho)\eta'(\rho).\end{aligned}$$

The first two terms on the above right hand side are non-positive, moreover

$$g'(\rho) \geq \frac{g(\rho)-g(\rho_L)}{\rho-\rho_L}$$

because of the concavity of g and in view of $\rho \leq \rho_L$. This proves the assertion.

Finally, we devote to case (d). In this case the turning point is located at a discontinuity having a classical shock x_L to its left hand side. An intermediate state ρ_m appears with $\rho_L^* = \rho_m$ and $\rho_R^* = \rho_R$. In order to validate such a structure, once again we have to match the Rankine–Hugoniot condition (41), the condition $\dot{x}_L < \dot{x}_M$, and (28) that reads in this case

$$\dot{x}_m(\eta(\rho_m)+\eta(\rho_R)) = \Psi^* - \dot{x}_L(\eta(\rho_L)-\eta(\rho_m)). \tag{42}$$

In order to check $\dot{x}_L < \dot{x}_m$, we need to prove

$$\frac{g(\rho_m)+g(\rho_R)}{\rho_R-\rho_m} + \frac{g(\rho_L)-g(\rho_m)}{\rho_L-\rho_m} > 0,$$

for $\rho_m \in [0,\rho_R)$, which is equivalent to

$$g(\rho_m)(\rho_L-\rho_R) + g(\rho_R)(\rho_L-\rho_m) + g(\rho_L)(\rho_R-\rho_m) > 0$$

which is trivially satisfied. Let us notice here that the case $\rho_m > \rho_R$ is incompatible with $\dot{x}_L < \dot{x}_M$, since the concavity of g would then imply

$$\dot{x}_m < -\frac{g(\rho_m)-g(\rho_R)}{\rho_m-\rho_R} < -\frac{g(\rho_m)-g(\rho_L)}{\rho_m-\rho_L} = \dot{x}_L$$

which is a contradiction.

Let us now check the compatibility between $\Psi^* > f(\rho_L)+f(\rho_R)$ and (42), which can be rewritten as

$$\lambda(\rho) := \frac{g(\rho)+g(\rho_R)}{\rho_R-\rho}(\eta(\rho)+\eta(\rho_R)) - \frac{g(\rho_L)-g(\rho)}{\rho_L-\rho}(\eta(\rho_L)-\eta(\rho)) = \Psi^*$$

with $\rho = \rho_m \in [0,\rho_R)$. It easily checked that

$$\lambda(0) = f(\rho_R)+f(\rho_L), \qquad \lim_{\rho\nearrow\rho_R}\lambda(\rho) = +\infty.$$

To conclude, it is enough to prove that $\lambda'(\rho) > 0$ for all $\rho \in [0,\rho_R)$. We notice that the function $\lambda(\rho)$ coincides with the function $-\theta$ defined in case (b) with the roles

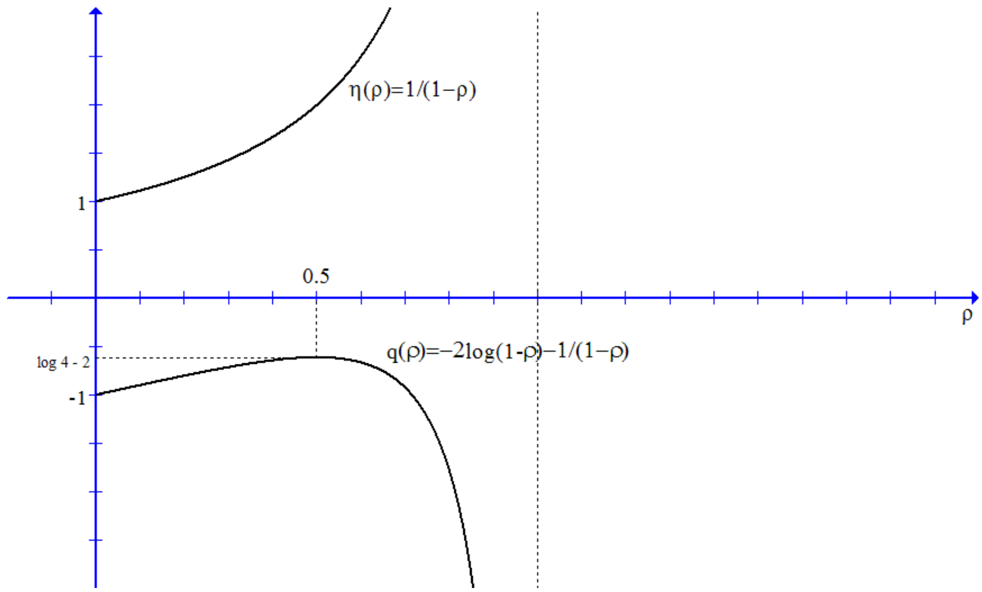

FIGURE 2. The function $\eta(\rho)$ and its flux $q(\rho)$, with $q(0) = -1$, in case $f(\rho) = 1 - \rho$.

of ρ_L and ρ_R inverted. Therefore, it is easy to compute

$$\begin{aligned}\lambda'(\rho) &\geq \frac{g(\rho)+g(\rho_R)}{\rho_R-\rho}\eta'(\rho)+\frac{g(\rho)-g(\rho_L)}{\rho-\rho_L}\eta'(\rho)\\ &= \eta'(\rho)\left\{\frac{g(\rho_R)}{\rho_R-\rho}+\frac{g(\rho_L)}{\rho_L-\rho}+g(\rho)\frac{\rho_R-\rho_L}{(\rho_R-\rho)(\rho-\rho_L)}\right\}.\end{aligned}$$

Since $\eta' > 0$, $g \geq 0$ and $\rho < \rho_R < \rho_L$, we conclude that $\lambda'(\rho) > 0$.

□

4. EXAMPLES

In this section we shall consider some examples in which the solution can be easily computed on the whole interval $[-1, 1]$, at least for small times. In some cases we shall provide a detailed description of the solution for all times, whereas in some other cases we shall describe the solution only qualitatively. By no means this section wants to explore all possible cases exhaustively. Our aim is just to show the occurrence of all the cases in Theorem 1 in explicit situations. For simplicity, we shall fix $f(\rho) = 1 - \rho$, which means η and q are as in Figure 2. In order to compute the term Ψ^* defined at the beginning of Section 3, we send the reader to Remark 3.

4.1. **Example: vacuum formation.** Let us consider the initial condition

$$\rho_0(x) \equiv 3/4, \qquad \text{for} \quad x \in [-1, 1].$$

It is clear that the solution will stay symmetric with respect to $x = 0$ and that $x_m(t) \equiv 0$ for all $t \geq 0$. Two rarefaction waves are generated at the boundary as in

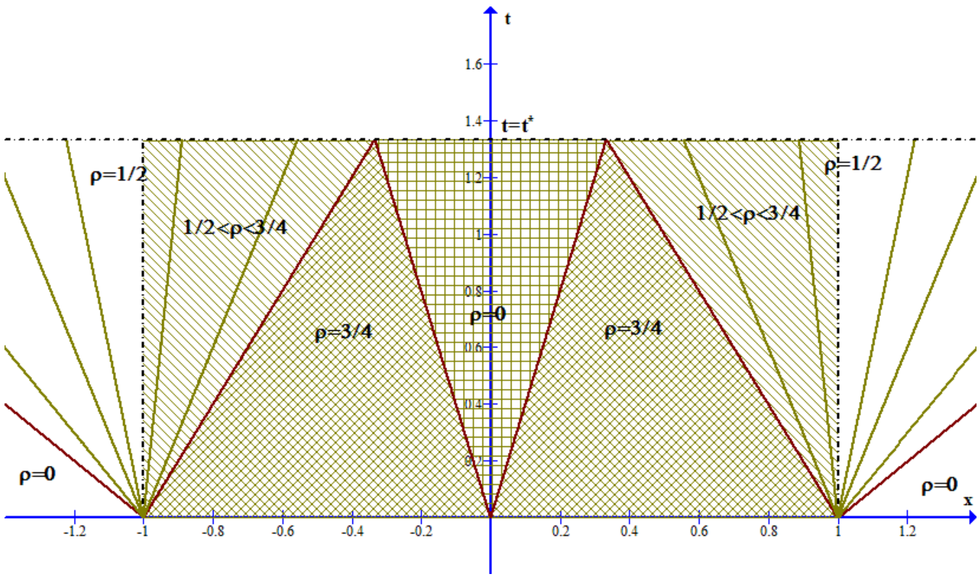

FIGURE 3. Solution with initial datum $\rho_0 \equiv 3/4$

figure 3. Away from the boundary, the characteristics are all converging towards $x = 0$, which could intuitively suggest that a solution is given by $\rho \equiv 3/4$ near the turning point. However, such choice does not satisfies the Rankine–Hugoniot condition in Proposition 2: the only possibility for a constant solution around the turning point is $\rho = 0$, i. e. a vacuum region is generated. This fact was already observed in the simulations performed in [16].

By using the notation in Section 3, we have in this case $\Psi^* = 0$ because of the initial symmetry. Therefore, with the notation of Theorem 1 we are in case (c), in which a decreasing shock connecting $3/4$ and 0 occurs on $x < 0$ and an increasing one between 0 and $3/4$ occurs on $x > 0$. Therefore, the unique entropy solution (for small times) is given by

$$\rho(t,x) = \begin{cases} \frac{x+1}{2t} + \frac{1}{2} & \text{if } -1 \le x < -1 + \frac{t}{2} \\ \frac{3}{4} & \text{if } -1 + \frac{t}{2} \le x < -\frac{t}{4} \\ 0 & \text{if } -\frac{t}{4} < x < \frac{t}{4} \\ \frac{3}{4} & \text{if } \frac{t}{4} \le x < 1 - \frac{t}{2} \\ \frac{1-x}{2t} + \frac{1}{2} & \text{if } 1 - \frac{t}{2} \le x \le 1. \end{cases}$$

The full characteristic plane is represented in figure 3. At time $t = t^* = \frac{4}{3}$ the two shock waves meet the two rarefaction waves coming from the boundary.

For $t > 4/3$ the problem can be solved as the in the classical case. The new shock curve on the left side is given by $x(t) = \sqrt{3t} - 1 - t$, see figure 3. Please notice that the solution becomes $\rho \equiv 0$ at the finite time $t = 3$.

4.2. **Example: Vacuum vs non-vacuum formation.** We consider the initial datum

$$\rho(x) = \begin{cases} \rho_1 & \text{if } -1 < x < 0 \\ \rho_2 & \text{if } 0 < x < 1\,, \end{cases} \tag{43}$$

with $0 \leq \rho_1 < \rho_2$. Then $\eta(\rho_1) < \eta(\rho_2)$ and therefore the initial turning point $x_m(0)$ defined in (19) is given by

$$x_m(0) = \frac{\eta(\rho_2) - \eta(\rho_1)}{\eta(\rho_2) + \eta(\rho_1)} = \frac{\rho_2 - \rho_1}{2 - \rho_1 - \rho_2} > 0.$$

In order to describe the behavior of the solution, we shall compute the function Ψ^* defined in Section 3 and compare it with the conditions in Theorem 1. Here $\rho_L = \rho_R = \rho_2$. We shall consider separate cases.

(1) $\rho_2 \leq 1/2$. The jump at $x = 0$ is solved by a rarefaction with minimal and maximal speeds given by $-1 + 2\rho_1 < 0$ and $-1 + 2\rho_2 < 0$ respectively. The traces at the boundary remain unchanged. Therefore,

$$\Psi^* = -q(\rho_2) + q(\rho_1)\,.$$

The assumption in case (c) of Theorem 1 holds if

$$q(\rho_2) \quad < \quad 2(1 - \rho_2) + q(\rho_1)\,, \qquad 0 \leq \rho_1 < \rho_2 \leq 1/2\,. \tag{44}$$

Since $q'(\rho) \geq 0$ for $\rho \in [0, 1/2]$, it is enough to prove (44) for $\rho_1 = 0$, that is for $x = \rho_2$

$$-2\log(1 - x) - \frac{1}{1 - x} \quad < \quad 1 - 2x\,, \qquad 0 \leq x \leq 1/2$$

which is trivially satisfied. Hence the solution has a vacuum around $x_m(t)$. The characteristic plane is as in Figure 4.

Once again, the shock–rarefaction interactions occurring here can be solved as in the classical case. The rarefaction wave is given by

$$\rho(t, x) = \frac{1}{2} + \frac{x}{2t} \qquad \text{on} \ \ (2\rho_1 - 1)t < x < (2\rho_2 - 1)t.$$

Its right front interacts with the shock wave $x = x_L(t)$ at time $t^* = \frac{x_m(0)}{\rho_2}$, thus originating a new shock curve $x_s(t) = 2\sqrt{\rho_2 x_m(0)}\sqrt{t} - t$. Clearly, the turning point is still located in a vacuum region $t = t^*$, therefore we can still apply Theorem 1 and compute Ψ^*. It is easy to check that the shock curve $x_R(t) = x_m(0) + (1 - \rho_2)t$ reaches the boundary later than t^*. In order to make sure that the turning point remains in the vacuum region for all times, we evaluate Ψ^* for $t > t^*$, here $\rho_L(t) = \rho(t, x_s(t))$:

$$\Psi^*[\rho](t) = -q(\rho_L(t)) + q(\rho_1) + \rho_L(t) - \rho_2,$$

for $t > t^*$ as long as the shock curve $x = x_R(t)$ does not reach the boundary. Due to $q'(\rho) > -1$ on $\rho \in [0, 1/2)$, it is easily seen that $\Psi^*[\rho](t) > \rho_1 - \rho_2$. This estimate also incorporates the times t after $x_R(t)$ has reached the boundary. Therefore, the turning point $x_m(t)$ remains in the vacuum region for all times and the solution becomes zero everywhere in a finite time.

(2) $1/2 < \rho_2 < 1/2(q(\rho_1) + 4 - \log 4)$. The rarefaction issued at $x = 0$ has a positive right speed, given by $-g'(\rho_2) = 2\rho_2 - 1$, and a rarefaction arises a $x = 1$

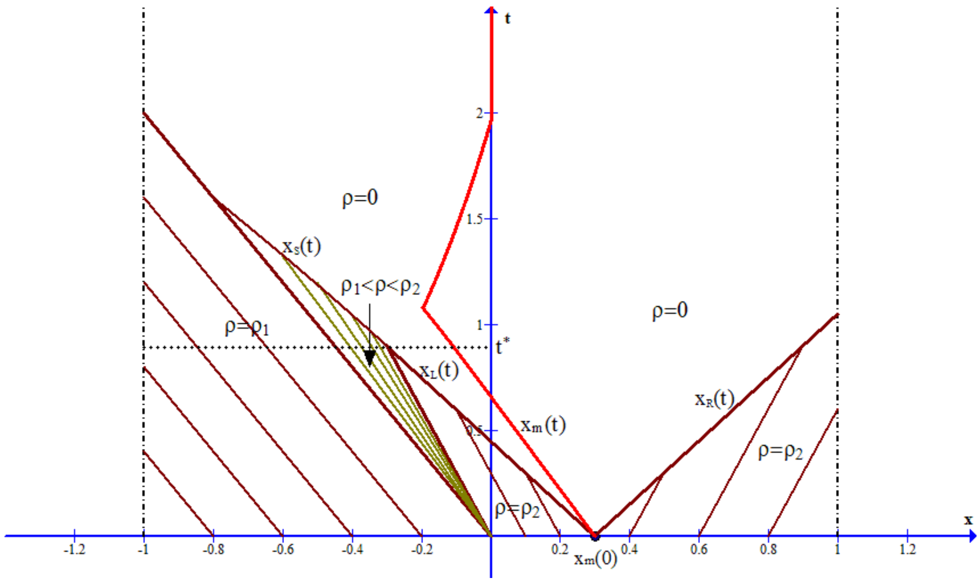

FIGURE 4. Characteristic plane for the Riemann problem with $0 < \rho_1 < \rho_2 < 1/2$

between ρ_2 and 1, because of the boundary condition. The computation of Ψ^* yields

$$\Psi^* = -q(1/2) + q(\rho_1),$$

and therefore the structure (c) in Theorem 1 is satisfied if

$$2\rho_2 \quad < \quad q(\rho_1) - q(1/2) + 2 \;=\; q(\rho_1) + 4 - \log 4\,.$$

Since $\rho_1 \in [0, 1/2]$, the above r.h.s. ranges in the interval $[3 - \log 4, 2]$, and this is compatible with our assumption on ρ_2. Therefore, a vacuum forms around $x_m(0)$. We omit the description for large times.

(3) $\rho_2 = 1/2(q(\rho_1) + 4 - \log 4)$. In this critical case, equality holds in the right inequality of (37), namely

$$\Psi^* = 2(\rho_2 - 1) = -2f(\rho_2).$$

A vacuum appears but this time the turning point $x_m(t)$ is located on a shock with ρ_2 and 0 as left and right states respectively.

(4) $1/2(q(\rho_1) + 4 - \log 4) < \rho_2 < 1$. In this case, as in the previous one, the vacuum cannot occur anymore around the turning point, and we must have a discontinuity arising at $x_m(0)$. Indeed, in this case

$$\Psi^* = q(\rho_1) - q(1/2) < -2f(\rho_2),$$

and we are therefore in case (b) of Theorem 1 with a strict inequality on the right hand side of (37). The statement (b) of Theorem 1 implies the existence of an intermediate value $\rho_m \in (0, \rho_2)$, within the fronts $x_m(t)$ and $x_R(t) = x_m(0) + \frac{g(\rho_2)-g(\rho_m)}{\rho_2-\rho_m}t$, see Figure 5. The dotted line in Figure 5 denotes the 'classical' shock curve one would have in case the turning point would still be located in a vacuum

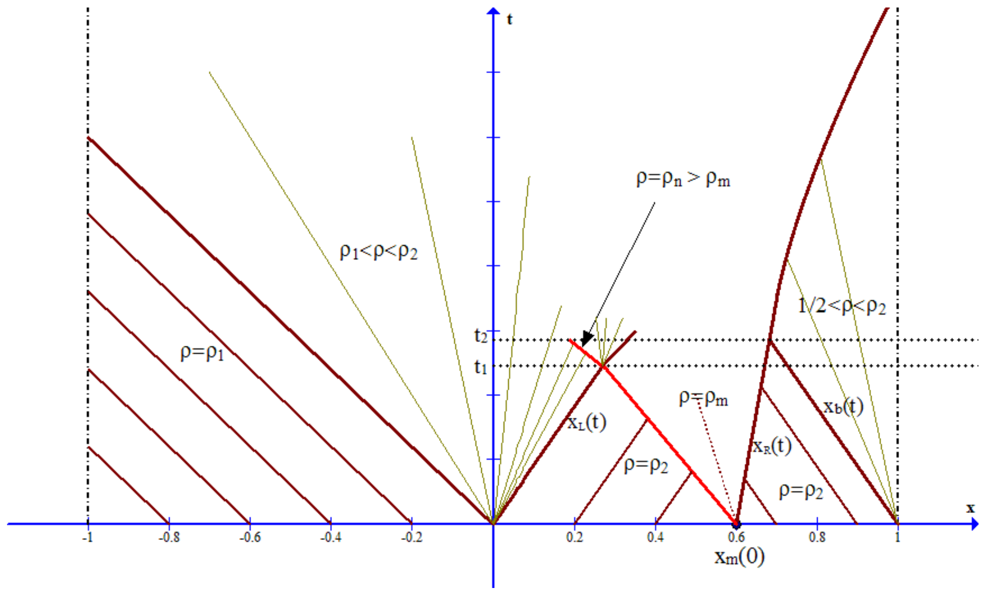

FIGURE 5. Characteristic plane for the Riemann problem with $0 < \rho_1 < \rho_2$ with $1/2(q(\rho_1) + 4 - \log 4) < \rho_2$

region: this time, x_m is initially too fast with respect to the two shock fronts, and thus the vacuum structure is not admissible. The right front of the rarefaction wave arising at $x = 0$ is $x_L(t) = (2\rho_2 - 1)t$, and the left front of the rarefaction wave arising at the boundary $x = -1$ is $x_b(t) = 1 - (2\rho_2 - 1)t$. It can be easily proven that the turning point curve $x_m(t)$ meets $x_L(t)$ at a time t_1 and $x_R(t)$ meets $x_b(t)$ at time t_2 with $t_1 < t_2$. Therefore, the relative evacuation rate at $t = t_1$ is

$$\Psi[\rho](t) = -q(\rho_L(t)) + q(\rho_1) + q(1/2) + q(\rho_2) + \dot{x}_R(t)(\eta(\rho_m) - \eta(\rho_2))$$

where $\rho_L(t) = \frac{1}{2} + \frac{x_L(t)}{2t} = \rho(t, x_L(t)-)$. Since the condition $1/2(q(\rho_1)+4-\log 4) < \rho_2$ implies $q(\rho_2) < q(\rho_L(t))$ (the condition implies $\rho_2 > 3/4$ and $q(3/4) < -1$, see figure 2), and assuming ρ_m small enough (it can be done by choosing ρ_2 close enough to $1/2(q(\rho_1) + 4 - \log 4)$) so to have $\dot{x}_R(t) > 0$, we are in the situation $\Psi[\rho](t_1) < \Psi^* < 0$. Therefore, (28) implies that $\dot{x}_m(t)$ has a decreasing jump after $t = t_1$. At this time one has to use (33) with a new right state ρ_n at $x = x_m(t)$ in order to match (28) with the Rankine–Hugoniot condition on x_m. Now, as $t \searrow t_1$ the difference quotient $(g(\rho_L(t))+g(\rho_n))/\rho_n-\rho_L(t)$ converges to $(g(\rho_2)+g(\rho_n))/\rho_n-\rho_2$. Since $\frac{g(\rho_2)+g(\rho)}{\rho-\rho_2}$ is non increasing as a function of ρ (see the proof or Proposition 2), then we have proven that $\rho_n > \rho_m$, which means that we are in a situation analogous to point (a) in Theorem 1: the turning point is located on a shock with $\rho_L(t)$ and ρ_n as left and right states respectively, whereas a new rarefaction wave arises on $x > x_m(t)$ connecting ρ_n with ρ_m. Since $\rho_L(t)$ is not constant in time, we expect the state ρ_n to be time dependent. The situation changes at $t = t_2$, in which the relative evacuation rate has to be re-computed. We omit the details.

(5) $1/2 < \rho_1 < \rho_2 < 1$. In this case, rarefaction waves arise form both boundary points thus implying $\Psi^* = 0$, which means that the turning point is initially constant. Then, a vacuum region appears around the turning point as in case (1).

Remark 5 (An interpretation in terms of mass transfer)**.** For a given solution $\rho(t,x)$ according to Definition 1, we define the *left mass* and the *right mass* of ρ as follows

$$M_L[\rho](t) := \int_{-1}^{x_m(t)} \rho(t,x)dx, \qquad M_R[\rho](t) := \int_{x_m(t)}^{1} \rho(t,x)dx.$$

It is clear that the total mass $M_L[\rho](t) + M_R[\rho](t)$ is strictly decreasing due to the boundary condition. In particular,

$$\frac{d}{dt}\left[M_L[\rho](t) + M_R[\rho](t)\right] = \frac{d}{dt}\int_{-1}^{1} \rho(t,x)dx = -g(\rho(t,1^-)) - g(\rho(t,-1^+)),$$

and one can compute the left and right *outgoing masses*

$$O_L[\rho](t) = \int_0^t g(\rho(\tau,-1^+))d\tau, \qquad O_R[\rho](t) = \int_0^t g(\rho(\tau,1^-))d\tau,$$

so that the total quantity $M_L + M_R + O_L + O_R$ is conserved in time. The question arises whether the two single quantities $M_L[\rho](t)+O_L[\rho](t)$ and $M_R[\rho](t)+O_R[\rho](t)$ are preserved in time. When this is the case, the two sets of pedestrians on the two sides of x_m lose mass because of the boundary conditions, but there is no mass transfer between the two sets. This is actually the case in the above situations (1) and (2): the two groups move away from the turning point and do not mix. This is due to the fact that the relative evacuation rate Ψ^* is not too big in absolute value, and the perception of the two boundary points at the turning point is not too different. In case (4), there is a mass transfer through the turning point. Indeed:

$$\begin{aligned}&\frac{d}{dt}\left[M_L[\rho](t) + O_L[\rho](t)\right] = g(\rho(t,x_m(t)^-)) + \dot{x}_m(t)\rho(t,x_m(t)^-)\\&= g(\rho_2) - \frac{g(\rho_2)+g(\rho_m)}{\rho_2-\rho_m}\rho_2 < 0\end{aligned}$$

where the last inequality is due to $\frac{g(x)+g(y)}{x-y} \in [(1-x),+\infty)$ for $x > y$. Similarly one can prove that $\frac{d}{dt}\left[M_L[\rho](t) + O_L[\rho](t)\right] > 0$. The interpretation is that the turning point moves towards the left side very quickly due to the very high (in absolute value) relative evacuation rate Ψ^*: in this case the pedestrians located at the turning point sense that the right boundary is getting much closer than the left boundary, and they are encouraged to cross the turning point in order to reach the right boundary.

Acknowledgments

MDF is partially supported by the grant MTM2011-27739-C04-02 of the Spanish Ministry of Science and Innovation, and supported by the 'Ramon y Cajal' Subprogramme (MICINN-RYC) of the Spanish Ministry of Science and Innovation, Ref. RYC-2010-06412.

References

[1] C. Bardos, A. Y. Leroux, and J. C. Nedelec. First order quasilinear equations with boundary conditions. *Comm. Partial Differential Equations*, 4:1017–1034, 1979.

[2] N. Bellomo and C. Dogbé. On the modelling crowd dynamics from scaling to hyperbolic macroscopic models. *Math. Models Methods Appl. Sci.*, 18(suppl.):1317–1345, 2008.

[3] F. Betancourt, R. Bürger, K. H. Karlsen, and E. M. Tory. On nonlocal conservation laws modelling sedimentation. *Nonlinearity*, 24:855–885, 2011.

[4] G. Bradley. A proposed mathematical model for computer prediction of crowd movements and their associated risks. *Smith, R.A., Dickie, J.F. (Eds.), Engineering for Crowd Safety. Elsevier, Amsterdam*, pages 303–311, 1993.

[5] A. Bressan. *Hyperbolic systems of conservation laws. The one-dimensional Cauchy problem*, Oxford University Press, 2000.

[6] A. Bressan and R. M. Colombo. P.D.E. models of pedestrian flow. Unpublished, 2007.

[7] M. Burger, P. A. Markowich, and J.-F. Pietschmann. Continuous limit of a crowd motion and herding model: analysis and numerical simulations. Preprint, 2011.

[8] G. Buttazzo, C. Jimenez, and E. Oudet. An optimization problem for mass transportation with congested dynamics. *SIAM J. Control Optim.*, 48:1961–1976, 2009.

[9] P. Cannarsa and C. Sinestrari. *Semiconcave Functions, Hamilton-Jacobi Equations, and Optimal Control*, volume 58 of *Progress in Nonlinear Differential Equations and Their Applications*. Birkhäuser.

[10] R. M. Colombo, M. Garavello, and M. Mercier. A class of non local models for pedestrian traffic. Preprint, 2011.

[11] R. M. Colombo and M. D. Rosini. Pedestrian flows and non-classical shocks. *Math. Methods Appl. Sci.*, 28(13):1553–1567, 2005.

[12] R. M. Colombo and M. D. Rosini. Existence of nonclassical solutions in a pedestrian flow model. *Nonlinear Anal. Real World Appl.*, 10(5):2716–2728, 2009.

[13] E. Cristiani, B. Piccoli, and A. Tosin. Multiscale modeling of granular flows with applications to crowd dynamics. *Multiscale Modeling and Simulations*, 9:155–182, 2011.

[14] C. M. Dafermos. Polygonal approximations of solutions of the initial value problem for a conservation law. *J. Math. Anal. Appl.*, 38:33–41, 1972.

[15] C. M. Dafermos. *Hyperbolic conservation laws in continuum physics*, Springer-Verlag, third edition, 2010.

[16] M. Di Francesco, P. A. Markowich, J.-F. Pietschmann, and M. T. Wolfram. On the Hughes' model for pedestrian flow: The one-dimensional case. *J. Differential Equations*, 250:1334–1362, 2011.

[17] C. Dogbé. Modeling crowd dynamics by the mean-field limit approach. *Mathematical and Computer Modelling*, 52:1506–1520, 2010.

[18] F. Dubois and P. LeFloch. Boundary conditions for nonlinear hyperbolic systems of conservation laws. *J. Differential Equations*, 71(1):93–122, 1988.

[19] M. Fukui and Y. Ishibashi. Self-organized phase transitions in CA-models for pedestrians. *J. Phys. Soc. Japan*, 8:2861–2863, 1999.

[20] D. Helbing. Traffic and related self-driven many-particle systems. *Rev. Mod. Phys.*, 73(4):1067–1141, Dec 2001.

[21] D. Helbing, I. J. Farkas, P. Molnar, and T. Vicsek. Simulation of pedestrian crowds in normal and evacuation situations. *In: M. Schreckenberg and S. D. Sharma (eds.)* Pedestrian and Evacuation Dynamics *(Springer, Berlin)*, pages 21–58, 2002.

[22] L. F. Henderson. The statistics of crowd fluids. *Nature*, 229:381–383, 1971.

[23] L. F. Henderson. On the fluids mechanics of human crowd motion. *Transp. Res.*, 8:509–515, 1974.

[24] R. L. Hughes. A continuum theory for the flow of pedestrians. *Transportation Research Part B: Methodological*, 36(6):507–535, 2002.

[25] R. L. Hughes. The flow of human crowds. *Annu. Rev. Fluid Mech.*, 35:169–182, 2003.

[26] R. A. Klausen and N. H. Risebro. Stability of conservation laws with discontinuous coefficients. *J. Differential Equations*, 157:41–60, 1999.

[27] S. N. Kružkov. First order quasilinear equations in several independent variables. *Math. USSR Sb*, 10:217–243, 1970.

[28] S. N. Kružkov. Generalized solutions of the Hamilton-Jacobi equations of eikonal type. i. formulation of the problems; existence, uniqueness and stability theorems; some properties of the solutions. *Math. USSR Sb.* 27, 1975.
[29] P. D. Lax. *Hyperbolic systems of conservation laws and the mathematical theory of shock waves.* CBMS Regional Conference Series in Applied Mathematics, No. 11. SIAM, Philadelphia, 1973.
[30] M. J. Lighthill and G. B. Whitham. On kinematic waves. ii. a theory of traffic flow on long crowded roads. *Royal Society of London Proceedings Series A*, 229:317–345, May 1955.
[31] B. Maury, A. Roudneff-Chupin, and F. Santambrogio. A macroscopic crowd motion model of the gradient-flow type. *M3AS*, 20:1787–1821, 2010.
[32] M. Muramatsu and T. Nagatani. Jamming transition in two-dimensional pedestrian traffic. *Physica A*, 275:281–291, 2000.
[33] O. A. Oleĭnik. Uniqueness and stability of the generalized solution of the Cauchy problem for a quasi-linear equation. *Uspehi Mat. Nauk*, 14(2 (86)):165–170, 1959.
[34] B. Piccoli and A. Tosin. Pedestrian flows in bounded domains with obstacles. *Contin. Mech. Thermodyn.*, 21(2):85–107, 2009.
[35] A. Schadschneider, W. Klingsch, H. Kluepfel, T. Kretz, C. Rogsch, and A. Seyfried. *Encyclopedia of Complexity and System Science*, R. A. Meyers, (ed.), Vol. 3, Chapter *Evacuation Dynamics: Empirical Results, Modeling and Applications*, Springer, 2009.
[36] G. Whitham. *Linear and Nonlinear Waves.* A Wiley & Sons, New York, 1974.

Debora Amadori, Dipartimento di Matematica Pura e Applicata, Università degli Studi dell'Aquila, via Vetoio, 1, 67010 Coppito L'Aquila, Italy
E-mail address: amadori@univaq.it

Marco Di Francesco, Departament de Matemàtiques, Universitat Autònoma de Barcelona, E-08193 - Bellaterra, Catalunya (Spain)
E-mail address: difrancesco@mat.uab.cat